\



Wavelength and sensitivity tunable long period gratings fabricated in fluid-cladding microfibers

Wa Jin(金娃), Linke Zhang(张林克), Xiang Zhang(张祥), Ming Xu(徐铭), Weihong Bi(毕卫红), and Yuefeng Qi(齐跃峰)

Citation: Chin. Phys. B, 2022, 31 (**1**): 014207. DOI: 10.1088/1674-1056/ac3394
Journal homepage: http://cpb.iphy.ac.cn; http://iopscience.iop.org/cpb

What follows is a list of articles you may be interested in

Photonic spin Hall effect and terahertz gas sensor via InSb-supported long-range surface plasmon resonance

Jie Cheng(程杰), Gaojun Wang(王高俊), Peng Dong(董鹏), Dapeng Liu(刘大鹏), Fengfeng Chi(迟逢逢), and Shengli Liu(刘胜利)

Chin. Phys. B, 2022, 31 (**1**): 014205. DOI: 10.1088/1674-1056/ac192a

Ultrabroadband mid-infrared emission from Cr^{2+}:ZnSe-doped chalcogenide glasses prepared via hot uniaxial pressing and melt-quenching

Ke-Lun Xia(夏克伦), Guang Jia(贾光), Hao-Tian Gan(甘浩天), Yi-Ming Gui(桂一鸣), Xu-Sheng Zhang(张徐生), Zi-Jun Liu(刘自军), and Xiang Shen(沈祥)

Chin. Phys. B, 2021, 30 (**9**): 094208. DOI: 10.1088/1674-1056/ac11eb

GaSb-based type-I quantum well cascade diode lasers emitting at nearly 2-μm wavelength with digitally grown AlGaAsSb gradient layers

Yi Zhang(张一), Cheng-Ao Yang(杨成奥), Jin-Ming Shang(尚金铭), Yi-Hang Chen(陈益航), Tian-Fang Wang(王天放), Yu Zhang(张宇), Ying-Qiang Xu(徐应强), Bing Liu(刘冰), and Zhi-Chuan Niu(牛智川)

Chin. Phys. B, 2021, 30 (**9**): 094204. DOI: 10.1088/1674-1056/abe930

Modeling of cascaded high isolation bidirectional amplification in long-distance fiber-optic time and frequency synchronization system

Kuan-Lin Mu(穆宽林), Xing Chen(陈星), Zheng-Kang Wang(王正康), Yao-Jun Qiao(乔耀军), and Song Yu(喻松)

Chin. Phys. B, 2021, 30 (**7**): 074208. DOI: 10.1088/1674-1056/abf105

Tunable wavelength filters using polymer long-period waveguide gratings based on metal-cladding directly defined technique

Ji-Hou Wang(王继厚), Chang-Ming Chen(陈长鸣), Yang Zheng(郑洋), Xi-Bin Wang(王希斌), Yun-Ji Yi(衣云骥), Xiao-Qiang Sun(孙小强), Fei Wang(王菲), Da-Ming Zhang(张大明)

Chin. Phys. B, 2017, 26 (**2**): 024212. DOI: 10.1088/1674-1056/26/2/024212

Wavelength and sensitivity tunable long period gratings fabricated in fluid-cladding microfibers

Wa Jin(金娃)[1,2,†], Linke Zhang(张林克)[2], Xiang Zhang(张祥)[2], Ming Xu(徐铭)[2], Weihong Bi(毕卫红)[1,2], and Yuefeng Qi(齐跃峰)[1,2]

[1] *Key Laboratory for Special Fiber and Fiber Sensor of Hebei Province, Qin Huangdao* 066004, *China*
[2] *School of Information Science and Engineering, Yanshan University, Qin Huangdao* 066004, *China*

(Received 4 August 2021; revised manuscript received 20 October 2021; accepted manuscript online 27 October 2021)

We report the fabrication of long period gratings in fluid-cladding microfibers by directly focusing a femtosecond laser beam on the microfibers surface to induce periodical modification a long one side of the microfibers. A long period grating is fabricated in a water-cladding microfiber with a diameter of ~ 5 μm, which demonstrates a resonant attenuation of 28.53 dB at wavelength of 1588.1 nm with 10 pitches. When water cladding is changed to be refractive index oil of $n = 1.33$ and alcohol solution with concentration of 5%, the resonance wavelength shifts to 1575.1 nm with resonant attenuation of 24.91 dB and 1594.1 nm with resonant attenuation of 35.9 dB, respectively. The long period grating demonstrates different temperature sensitivities of -0.524 nm/°C, -0.767 nm/°C and -1.316 nm/°C for water, alcohol solution and refractive index oil cladding microfibers, respectively, which means the alterable liquid cladding allows the availability of tunable wavelength and sensitivity. The fluid-cladding protects the microfibers from external disturbance and contamination and allows more flexibility in controlling the transmission property and sensing characteristics of long period gratings, which can be used as fiber devices and sensors for chemical, biological, and environmental applications.

Keywords: fluid-cladding microfiber, long-period grating, temperature

PACS: 42.81.–i, 42.81.Pa, 42.81.Bm **DOI:** 10.1088/1674-1056/ac3394

1. Introduction

A long-period grating in a single-mode fiber demonstrates a resonance at a specific wavelength in the transmission spectrum by coupling energy from the fundamental mode to the cladding mode of the fiber. However, the geometry and material constraints of conventional fiber impose significant limitations on the functions that a long-period grating can achieve.[1] For example, it is difficult to realize a widely tunable filter at room temperature and highly sensitive sensor. To design a wavelength tunable long-period grating, some configurations are proposed, such as applying mechanical pressure to a long-period holey-fiber grating,[2] temperature to a complicated fiber structure containing air rings in the cladding filled with polymer[3] and fabricating a long-period grating in a B–Ge doped fiber by a careful choice of a high-order cladding mode,[4] however, the wavelength tunability is not permanent because the wavelength shift disappears without the changed environment.

The phase matching condition of a long-period grating is given by $\lambda_{\rm res} = \Lambda \left| n_{{\rm eff},o} - n_{{\rm eff},m} \right|$, where $\lambda_{\rm res}$ is the resonance wavelength, Λ is the grating pitch, and $n_{{\rm eff},o}$ and $n_{{\rm eff},m}$ are the effective refractive indices of the two coupled modes.[5] The phase matching condition depends on the effective refractive index difference between these two modes, hence the resonant wavelength $\lambda_{\rm res}$ can be made to be very sensitive to small changes in $n_{\rm eff}$ through proper design of the optical fibers, thus the resonant wavelength of the long-period gratings can be widely tunable to very small changes in ambient environment,[6] which is the potential applications of microfibers. Microfiber has attracted significant attention due to a large evanescent field outside the fiber, which allows strong evanescent-wave coupling between microfibers and their environment[7,8] and can induce high tunability of the optical property of the fiber and high sensitivity in optical fiber sensing field.[9–11] However, the optical performances of the conventional microfiber long period grating and microhole fiber long period grating degrade quickly due to light scattering from dust particles and cracks induced by water vapor, and an increasing unrecoverable optical loss is observed over time if they are left in open air.[12,13] Moreover, the microfibers are fragile and not easy to handle, which hinders practical applications of these fibers.

In this paper, a fluid-cladding microfiber is proposed to achieve the wavelength tunability of long-period gratings by changing the fluid material of cladding directly at room temperature, which avoids changing temperature, applying mechanical pressure and inducing complicated operation on the fiber, and is more practical for real-world applications. A long-period grating in water cladding microfiber is fabricated by scanning a focused femtosecond infrared laser periodically across the surface of the microfiber, which demonstrates a resonant attenuation of 28.53 dB with 10 pitches at wavelength of 1588.1 nm. When the cladding material of water is changed

†Corresponding author. E-mail: jinwa@ysu.edu.cn

© 2022 Chinese Physical Society and IOP Publishing Ltd

to alcohol solution with concentration of 5% and refractive index oil of $n = 1.33$, the resonance wavelength of the long-period grating shifts to 1594.1 nm with resonant attenuation of 35.9 dB and 1575.1 nm with resonant attenuation of 24.91 dB, respectively. To illustrate the flexible sensing applications of this fluid cladding microfiber long-period grating, temperature sensing characteristics of these three different cladding microfiber long-period gratings are measured, which demonstrate different sensitivities of -0.524 nm/°C, -0.767 nm/°C and -1.316 nm/°C, respectively.

2. Experimental results and discussion

The microfiber is fabricated by bi-tapering a conventional single mode fiber. A laboratory flame taper machine with movable flame is setup in our experiment to fabricate a microfiber with long uniform length, as shown in Fig. 1. The two pigtails of a single mode fiber are mounted on two three-axis translation stages, and a hydrogen flame with a diameter of 10 mm is used to heat and soften the fiber. The flame is scanning along the fiber back and forth with a scan length of L and a velocity of V_S, while the two translation stages move in the opposite direction with the same velocity V_P. This lab-made machine can draw a microfiber with uniform length of 8 cm and diameter of ~ 1 μm.

A 5 cm-long and ~ 5 μm-diameter microfiber is used in our experiment, which is inserted into a capillary tube. The microfiber is kept straight and suspended along the center line of the capillary tube while its single mode fiber pigtails are glued to the two ends of the capillary. The capillary used in our experiment has inner and outer diameters of ~ 660 μm and ~ 900 μm, respectively. During the process of tapering and encapsulation, the transmission spectrum of the microfiber is monitored by connecting the input and output single mode fiber pigtails respectively to a broadband light source and an optical spectrum analyzer, and a large transmission loss is observed if the microfiber is broken or adhered to the inner wall of the capillary. A loss of ~ 0.2 dB is achieved with a capillary containing the microfiber, which shows that the encapsulation does not change the optical property of the microfiber but the capillary tube protects the microfiber from external disturbance and contamination and makes it more robust.

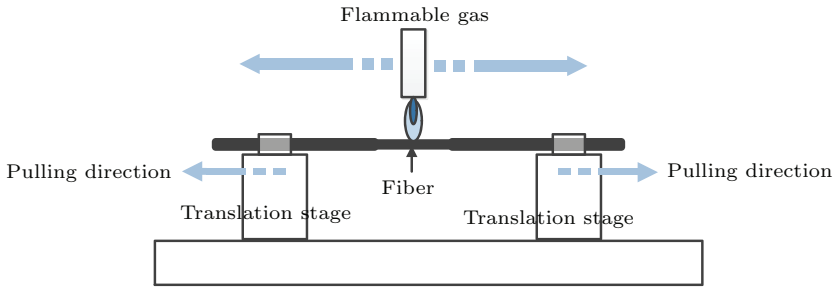


Fig. 1. Schematic figure of lab-made taper machine.

Two side holes are drilled on the capillary wall, which act as ingress/egress channels for sample fluids. One hole on the capillary wall is immersed into water while the other hole is left open to the air, and the section between the two side-holes is filled with water in a few seconds via capillary effect, as shown in the inset of Fig. 2. Such structure is robust and stable, and can be easily integrated into standard fiber-optic circuits with low loss, making the fluid cladding microfiber-based devices more practical for real-world applications.

The LPG is fabricated by a point-by-point technique. The encapsulated liquid cladding microfiber is mounted on two computer-controlled three-dimension translated stages. The input and output pigtails of the single mode fiber from which the microfiber is made are connected respectively to a broadband light source and an optical spectrum analyzer. Femtosecond laser pulse is focused on the upper surface of a microfiber, and the irradiation intensity and diameter of the focal spot are respectively ~ 0.15 J/cm^2 and 3 μm. The fabrication process is as following: firstly, the laser beam scans the microfiber transversely to fabricate the first point, then the focal spot moves longitudinal with a period to induce the second point, and the transmission spectrum of the long-period grating is monitored during fabrication process, as shown in Fig. 2. What we want to show here is that the long-period grating is directly fabricated in the fluid cladding microfibers by adjusting the focus and the energy of the femtosecond laser pulse, regardless of the capillary tube that encapsulates the microfiber and the fluid surrounding the microfiber. The encapsulation has little or no effect on the inscription. The red line in Fig. 3 shows the transmission spectrum of a long-period grating made on an encapsulated microfiber with water cladding. The resonant wavelength is 1588.1 nm, and the strength of the attenuation dip is 28.53 dB.

To change the cladding material, the water is removed and cleared, and a new fluid material is filled into the same capillary tube. By use of a piece of absorbent paper to cover one of the holes on the capillary wall, the majority of water within

the capillary can be removed within few seconds. The tube is then re-filled with 99.5% propyl alcohol to clean the left water fluid, which is removed by placing the absorbent paper on the hole. This process is repeated a number times and the capillary left in air for a few minutes to dry out the alcohol. Then the capillary tube is filled with 5% propyl alcohol solution, and a new long-period grating appears. The new resonance wavelength is 1594.1 nm, and the attenuation dip is 35.9 dB. When the cladding material is changed to a refractive index oil with $n = 1.33$, the long-period grating shows resonance wavelength of 1575.1 nm and attenuation dip of 24.91 dB, as shown in Fig. 3.

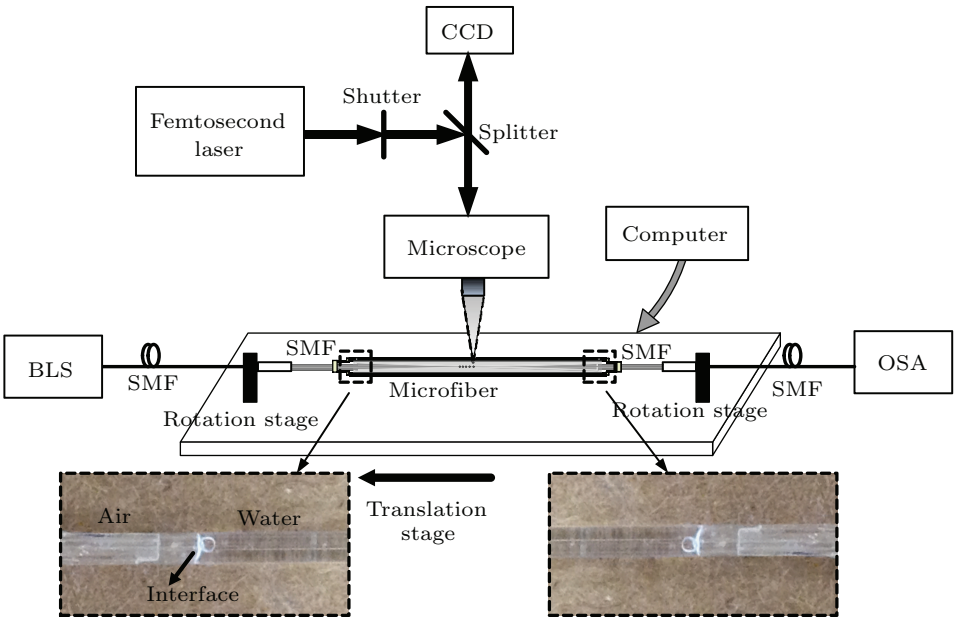


Fig. 2. Experimental setup for fabrication long-period grating in water cladding microfiber with femtosecond laser. Inset: picture of the two ends of the capillary.

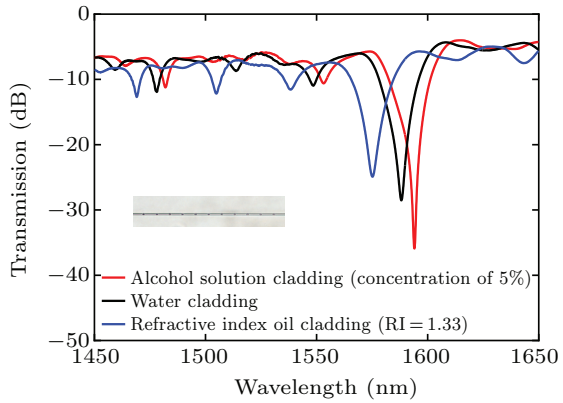


Fig. 3. Transmission spectra of long-period grating fabricated in microfibers with different kinds of fluid cladding. Inset: microscope image of long-period grating.

The modal property of microfibers with different claddings is studied by using a three-layer (a circular core, a circular silica rod with a fluid cladding) step-index model. Figure 4 demonstrates the mode property of the microfiber with water cladding. It is obviously that the microfiber with water cladding can support few guided modes, and hence a long-period grating is fabricated by coupling between the fiber modes.

The resonant wavelength in the long-period grating can be obtained through the expression $\lambda_{\text{res}} = \Lambda \left| n_{\text{eff}x} - n_{\text{eff}y} \right|$. In the case of a fluid cladding microfiber, the resonant wavelength for which coupling condition is satisfied depends on the fluid cladding material which induces different effective refractive indices of fundamental mode HE_{11} and high order mode HE_{21}.

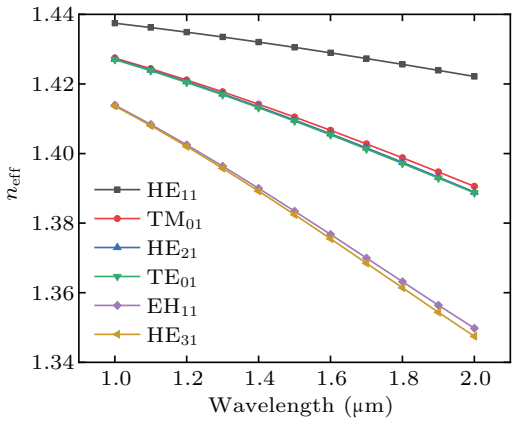


Fig. 4. Guided modes in water cladding microfiber.

Based on the above equation, the phase-matching curves corresponding to the resonant coupling between the fundamental and the first group of higher-order modes with different fluid claddings are calculated for a microfiber with diameter of 5 μm and shown in Fig. 5. For a grating pitch of 70 μm, Fig. 5 predicts that three resonance dips of the three different fluid cladding microfibers would be formed around 1530 nm, 1543.6 nm, and 1550 nm, corresponding to cou-

pling from HE_{11} to HE_{21} for refractive index oil cladding microfiber, water cladding microfiber, and 5% propyl alcohol solution cladding microfiber, respectively. The transmission spectrum matches well with the calculated results for HE_{11}–HE_{21} coupling with a pitch of 68.7 μm, the difference between the theoretical result and the experimental result may come from the little measurement deviation of diameter of the microfibers.

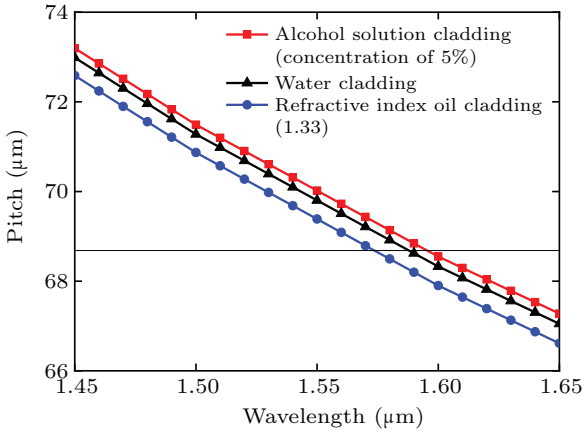


Fig. 5. Phase matching curves for microfibers with different fluid claddings.

As can be seen from Fig. 6, the refractive index difference between fundamental mode HE_{11} and higher-order mode HE_{21} in a microfiber becomes much larger with the diameter of the microfiber decreasing, thus the pitch achieving the phase match condition becomes much smaller, for example, when the refractive index of liquid cladding is 1.3, the pitch is about 30 μm for the microfiber to achieve resonant wavelength of 1550 nm, while it is about 92 μm for the same cladding microfiber with diameter of 6 μm to achieve the same coupling. The resonant wavelength shifts to the longer wavelength with the refractive index of the liquid cladding increasing for the same microfiber, and the tunable range is much wider with the decrease of the diameter of the microfiber, for example, the resonant wavelength of 1.31 μm shifts to 1.59 μm for the microfiber with a diameter of 3 μm when the refractive index of the liquid cladding changes from 1.3 to 1.33, while the resonant wavelength of 1.51 μm shifts to 1.58 μm when the diameter of the microfiber is 6 μm. The tunable wavelength spans are 280 nm and 70 nm, respectively. The diameter and the flexible cladding make the tunable resonant wavelength of long-period grating fabricated in liquid cladding microfiber available.

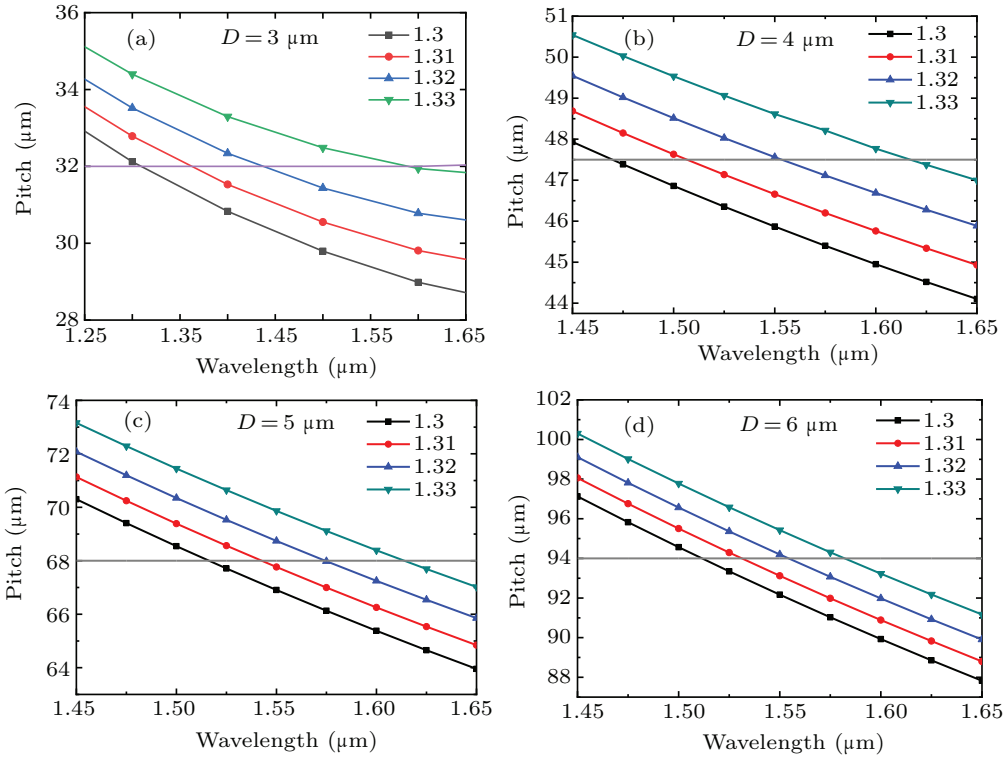


Fig. 6. Phase matching curves for different refractive index fluid cladding microfibers with different diameters: (a) 3 μm, (b) 4 μm, (c) 5 μm, (d) 6 μm.

3. Sensing characteristics

The physical property of fluid cladding of microfiber can be used for sensing applications. The transmission spectra of this microfiber with different fluid cladding are monitored when the surrounding temperature is varied from room temperature to 45 °C by use of a digital controlled oven. The resonance dips shift to short wavelength with the temperature increase, and the measured spectrum of the long-period grating fabricated in microfiber with water cladding is shown in Fig. 7(a). Different temperature sensitivities are achieved,

−0.524 nm/°C, −0.767 nm/°C, and −1.316 nm/°C, respectively, corresponding to the long-period gratings fabricated in the same microfiber with water cladding, alcohol solution cladding, and refractive index oil cladding, respectively, as shown in Fig. 7(b), which is higher than that of the other sensors, as shown in Table 1.

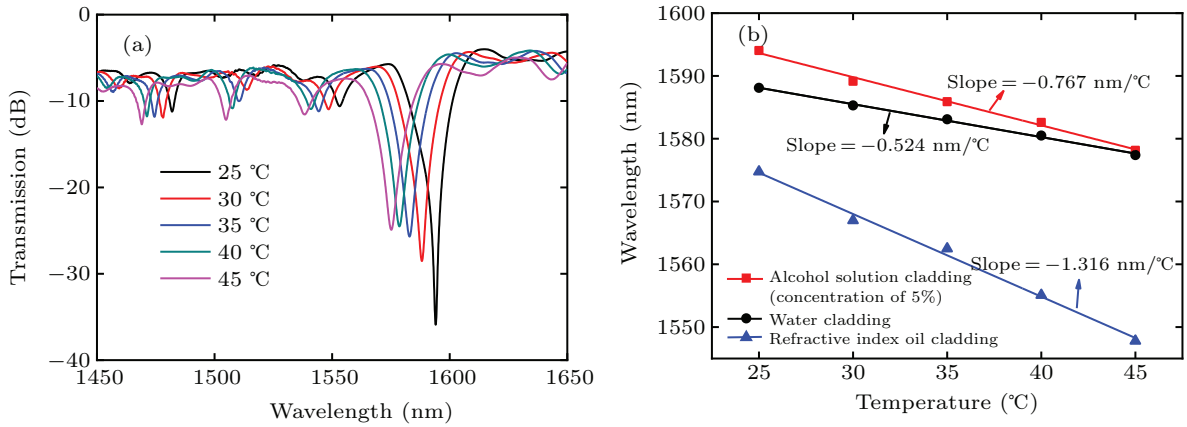


Fig. 7. (a) Spectra evolution of long-period grating fabricated in water cladding microfiber. (b) Resonant wavelength as a function of temperature for different fluid cladding microfiber long-period gratings.

Table 1. Comparison of temperature sensitivities for different sensors.

References	Structure	Sensitivity (nm/°C)
[14]	no-core fiber	–0.183
[15]	Michelson interferometer	0.12
[16]	Fabry–Perot interferometer	0.17930
[17]	microfiber FBG	0.0265
[18]	microfiber ring	–0.04158
This paper	liquid cladding microfiber long-period grating	–1.316

The sensitivity (S) of the resonant wavelength (λ) to temperature (T) of the long period grating is expressed as

$$\frac{\mathrm{d}\lambda_{\mathrm{res}}}{\mathrm{d}T} = \left(\frac{\mathrm{d}n_{\mathrm{eff},o}}{\mathrm{d}T} - \frac{\mathrm{d}n_{\mathrm{eff},m}}{\mathrm{d}T}\right)\Lambda + (n_{\mathrm{eff},o} - n_{\mathrm{eff},m})\frac{\mathrm{d}\Lambda}{\mathrm{d}T}, \quad (1)$$

where λ_{res} is the resonance wavelength, Λ is the grating pitch, T is the temperature, $n_{\mathrm{eff},o}$ and $n_{\mathrm{eff},m}$ are respectively the effective refractive indices of the fundamental mode and the m-order mode, $\mathrm{d}\Lambda/\mathrm{d}T$ is the change of pitch with temperature, which can be ignored in our experiment because the Ge-doped region of the microfiber is so small that it can be considered as a pure silica fiber and the difference of thermal expansion between the Ge-doped region and the silica cladding can be ignored. The sensitivity can be expressed as

$$\frac{\mathrm{d}\lambda_{\mathrm{res}}}{\mathrm{d}T} = \left(\frac{\mathrm{d}n_{\mathrm{eff},o}}{\mathrm{d}T} - \frac{\mathrm{d}n_{\mathrm{eff},m}}{\mathrm{d}T}\right)\Lambda = \lambda_{\mathrm{res}} \cdot \gamma \cdot \Gamma_{\mathrm{temp}}, \quad (2)$$

where γ is the waveguide dispersion factor and expressed as

$$\gamma = \frac{\frac{\mathrm{d}\lambda_{\mathrm{res}}}{\mathrm{d}\Lambda}}{n_{\mathrm{co}}^{\mathrm{eff}} - n_{\mathrm{cl},m}^{\mathrm{eff}}}. \quad (3)$$

The Γ_{temp} is the temperature sensitive factor and expressed as

$$\Gamma_{\mathrm{temp}} = \frac{\xi_{\mathrm{co}} n_{\mathrm{co}}^{\mathrm{eff}} - \xi_{\mathrm{cl}} n_{\mathrm{cl},m}^{\mathrm{eff}}}{n_{\mathrm{co}}^{\mathrm{eff}} - n_{\mathrm{cl},m}^{\mathrm{eff}}}, \quad (4)$$

where ξ_{co} and ξ_{cl} are the thermo-optical coefficients of core and cladding, respectively.

The water cladding microfiber is taken as an example, the resonant wavelength as a function of pitch is shown in Fig. 8 under HE_{11} and HE_{21} coupling. It is obviously that when $\mathrm{d}\lambda_{\mathrm{res}}/\mathrm{d}\Lambda > 0$ the diameter of the fiber is smaller than 2 μm, $\mathrm{d}\lambda_{\mathrm{res}}/\mathrm{d}\Lambda < 0$ when the diameter of the fiber is larger than 3 μm, and $\mathrm{d}\lambda_{\mathrm{res}}/\mathrm{d}\Lambda$ is turned from positive to negative when the diameter is increased from 2 μm to 3 μm. The similar analysis can be conducted for refractive index oil cladding and alcohol solution cladding.

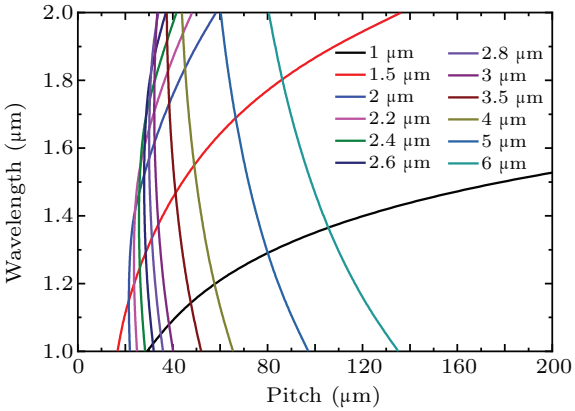


Fig. 8. Resonant wavelength as a function of pitch.

Thus the sensitivity as a function of normalized diameter (D/λ) for water cladding,alcohol solution cladding and refractive index oil cladding is calculated as shown in Fig. 9, and the theoretical sensitivities are −0.588 nm/°C, −0.61 nm/°C and

−1.06 nm/°C shown in the inset of Fig. 9, respectively. The experimental results are in good agreement with the theoretical results, and the little difference comes from the microfiber diameter measurement error and the little thermo-optical coefficient difference between theoretical data and actual data.

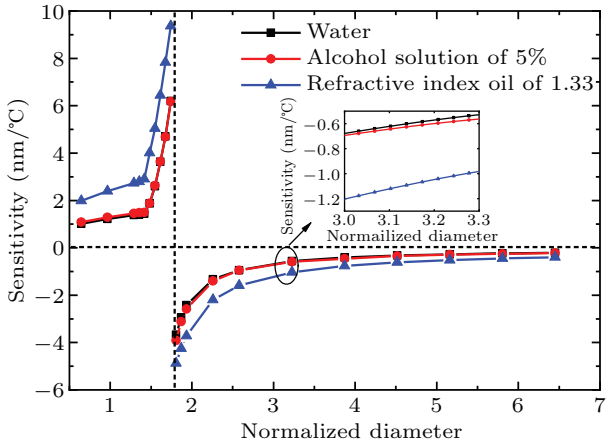


Fig. 9. Sensitivity as a function of normalized diameter. Inset is sensitivity as a function of normalized diameter of 3.0 to 3.3.

4. Conclusion

We reported a simple wavelength and sensitivity tunable long-period grating fabricated in a fluid-cladding microfiber. A long-period grating in water cladding, refractive index oil cladding and alcohol solution cladding microfiber demonstrated a resonant attenuation of 28.53 dB at wavelength of 1588.1 nm, 24.91 dB at wavelength of 1575.1 nm, and 35.9 dB at wavelength of 1594.1 nm, respectively, which are used for temperature measurement with different sensitivities. The alterable cladding material makes possible the realization of ultra wide-band tunable filters and variable sensors for different applications. We can envisage many new applications such as low loss evanescent-wave-coupled optical absorption, amplification, florescence, Raman and photoacoustic cells with this fluid cladding microfiber long-period grating by exploitation of many materials available for microfiber cladding. Realization of active devices and environmental sensors looks particularly promising.

Acknowledgements

Project supported by the National Natural Science Foundation of China (Grant Nos. 61605168 and 61735011), the Natural Science Foundation of Hebei Province, China (Grant Nos. F2016203392 and F2021203058), the College and University Science and Technology Research Project of Hebei Province, China (Grant No. QN2016078), and the Intramural Doctoral Foundation of Yanshan University (Grant No. B1011).

References

[1] Chiang K S, Lor K P, Chow C K, Chan H P, Rastogi V and Chu Y M 2003 *IEEE Photonics Technology Letters* **15** 1094

[2] Ceballos Herrera D E, Torres Gómez I, Martínez Ríos A, Anzueto Sánchez G, Alvarez Chávez J A, Selvas Aguilar R and Sánchez Mondragón J J 2007 *Appl. Opt.* **46** 307

[3] Kwon M S and Shin S Y 2014 *IEEE Photonics Technology Letters* **17** 145

[4] Shu X W, Allsop T, Gwandu B, Zhang L and Bennion I 2001 *IEEE Photonics Technology Letters* **13** 818

[5] Janczuk Richter M, Dominik M, Roźniecka E, Koba M, Mikulic P, Bock W J, Marcin Łoś, Mateusz Śmietana and Joanna Niedziółka Jönsson 2017 *Sensors & Actuators B Chemical* **250** 32

[6] Yu C B, Wu Y, Liu X L, Yao B C, Fu F, Gong Y, Rao Y J and Chen Y F 2016 *Optical Materials Express* **6** 727

[7] Li J, Li M M, Sun L P, Fan P C, Ran Y, Jin L and Guan B O 2017 *Acta Phys. Sin.* **66** 074209 (in Chinese)

[8] Villatoro J and Monzónhernández D 2005 *Opt. Express* **13** 5087

[9] Cao Y, Pei Y W and Tong Z R 2014 *Acta Phys. Sin.* **63** 024206 (in Chinese)

[10] Sumetsky M 2008 *Journal of Lightwave Technology* **26** 21

[11] Tong L M, Lou J Y, Gattass R R, He S L, Chen X W, Liu L and Mazur E 2005 *Nano Lett.* **5** 259

[12] Xiao L, Grogan M D W, Wadsworth W J, England R and Birks T A 2011 *Opt. Express* **19** 764

[13] Xu F and Brambilla G 2008 *Jpn. J. Appl. Phys.* **47** 6675

[14] Sun J C, Wang T T, Dai Y, Chang J H and Ke W 2021 *Acta Phys. Sin.* **70** 064202 (in Chinese)

[15] Yang S, Rong Q Z, Sun H, Zhang J, Liang L, Xu Q F, Zhan S C, Du Y Y, Feng D Y, Qiao X G and Hu M L 2013 *Acta Phys. Sin.* **62** 084218 (in Chinese)

[16] Yang Y, Xu B, Liu Y M, Li P, Wang D N and Zhao C L 2017 *Acta Phys. Sin.* **66** 094205 (in Chinese)

[17] Yang S, Daniel H, Gary P and Wang A B 2018 *Opt. Lett.* **43** 62

[18] Liu Z L, Xiao H F, Liao M M, Han X, Chen W P, Zhao T, Jia H, Yang J H and Tian Y H 2019 *IEEE Photonics Technology Letters* **31** 337